1 Introduction

1.1 A short history of exoplanets

In this thesis our goal is to model the broadband polarimetric signal of exoplanets containing various forms of inhomogeneities, like for example continents and oceans, hazes, clouds etc. Some of these inhomogeneities, like water clouds in a planetary atmosphere are very important for the existence of life as we know it, and as we will see in this thesis tend to leave a characteristic signal on the planetary signal.

Man kind has been pondering for centuries over the possible existence of exoplanets, i.e. planets that orbit around a star other than our Sun, that could harbor life. Already in ancient Greece, philosophers like Democritus and Epicurus were speaking of the existence of infinite worlds, either like or unlike ours.

> *"In some worlds there is no Sun and Moon, in others they are larger than in our world, and in others more numerous. In some parts there are more worlds, in others fewer (...); in some parts they are arising, in others failing. There are some worlds devoid of living creatures or plants or any moisture."* - Democritus (460–370 B.C.)

Aristotle's authority and opinion that there "cannot be more worlds than one", shadowed any further advancement on the topic for centuries. Giordano Bruno and a couple of centuries later Christiaan Huygens among others will come back to this topic, and claim the existence of multiple worlds like ours.

> *"Why should not every one of these stars or suns have as great a retinue as our sun, of planets, with their moons, to wait upon them?"*
> *- Christiaan Huygens (1629–1695 A.D.)*

Huygens performed the first documented effort to detect exoplanets (Κοσμοθεωρός, 1698). Any efforts though to detect exoplanets back then would be futile

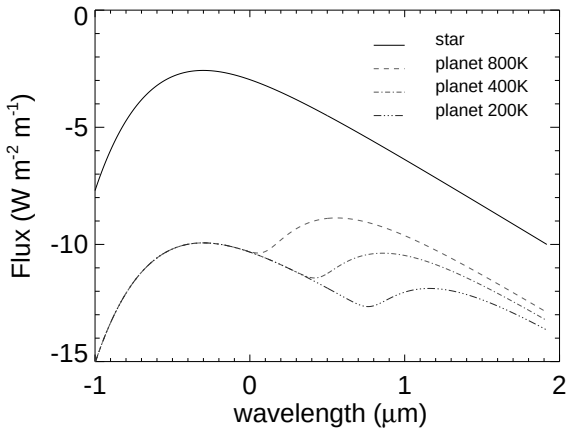

Figure 1.1: Solar flux of a Sun–like star as a function of the observation wavelength. The Star is set 4pc away from the observer. Over–plotted are the fluxes of a Jupiter–like planet lying 1A.U. from its parent star with a temperature of 200K (blue, dashed–triple–dotted line), 400K (green, dashed–dotted line) or 800K (red, dashed line). For giant planets the planet to star contrast ratio is of the order of 10^{-9}, while for terrestrial planets this ratio can be of the order of 10^{-11} in the visible.

since exoplanets are so faint in comparison to their parent stars (see Fig. 1.1) that with the means of that time their detection was impossible.

Some centuries later, astronomer P. van de Kamp using astrometry found a wobble in Barnard's star motion which he attributed to the existence of initially one and later two giant planets (van de Kamp 1969b,a). His findings have not been reconfirmed so far. The first official discovery of an exoplanet was done by Wolszczan & Frail (1992) who discovered an exoplanet orbiting around a pulsar. A pulsar – a highly magnetised, rotating neutron star that emits a beam of electromagnetic radiation – is not the ideal parent star for astronomers that seek our Earth's twin planet, but nevertheless this was the first time that the idea of the existence of planets outside our Solar System was reconfirmed.

A couple of years later the discovery of the first exoplanet orbiting a solar–like star by Mayor & Queloz (1995) inaugurated a new era in astronomy. In the less than two decades that have followed that discovery, more than 770 exoplanets have been detected up to today (source: The extrasolar planets encyclopedia). As we

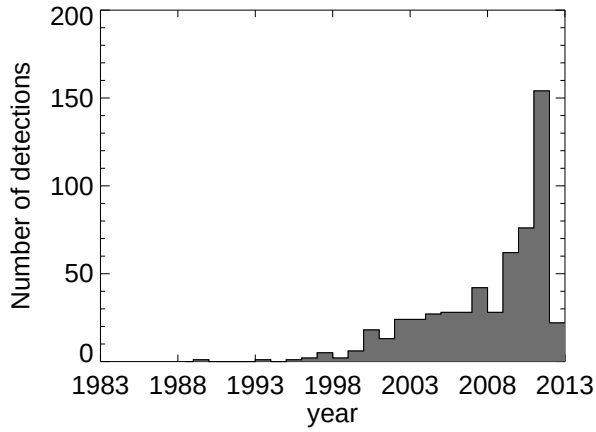

Figure 1.2: Number of exoplanets detected per year from 1983 up to 2012. As we can see, the number of exoplanet detections has been increasing almost exponentially in the past years thanks to instruments like HARPS, COROT and Kepler.

can see in Fig. 1.2 the number of exoplanet detections per year increases almost exponentially, mostly due to the improved instruments and detection techniques.

1.2 Detection methods of exoplanets

Since the first discovery of the first exoplanet orbiting a solar–like star by Mayor & Queloz (1995), using the radial velocity method a number of techniques have been developed for the detection and characterization of exoplanets. Most of these techniques are indirect, i.e. we never detect/ observe the planet itself, but we see the effect its existence has on the signal of its parent star. Here, we briefly present some of these techniques and the amount of information we can acquire with each one. Finally, in Table 1.1 we present the number of exoplanets detected with each method so far.

1.2.1 Indirect detection of exoplanets

The **radial velocity** (RV) method is the oldest technique used for the detection of exoplanets. It is to this technique that we owe the detection of the first exoplanet

orbiting a solar–like star (Mayor & Queloz 1995) and the start of the field of exoplanetary research. The RV method is based on the study of the Doppler shift of the parent star's light due to the rotation of the planet around it. The method is mostly sensitive to massive stars orbiting close to their parent star, since these planets have the largest radial velocities. Additionally, large orbits will require large observation times. Even though we owe the largest number of planetary detections to this method, we are close to reaching its limits.

The **planetary transit** method is the new method to which we owe a large number of exoplanet detections, and which is rapidly catching–up with the RV method thanks to new, space–born instruments like COROT (Convection, ROtation & planetary Transits) (Baglin et al. 2006) and Kepler (Koch et al. 1998). This method is based on measuring the dimming of the emitted light from the parent star as the planet transits, i.e. passes in front of the stellar disk, covering it partially and allowing less starlight to arrive to the observer. This method is sensitive to large planets that orbit close to their parent star[1]. These biases of the planetary transit method are the another reason why most of the exoplanets detected up to today are so–called hot Jupiters and not Earth–like planets.

Finally, the **microlensing** method uses the gravitational lensing phenomenon for the detection of exoplanets (Gould & Loeb 1992). When a foreground star passes close to the line of sight of a distant, background star, the foreground star will act as a lens and split the light of the background star in two, usually unresolved images. If the foreground star hosts a planet, whose plane of rotation lies close to the plane of observation, the latter will also act as a lens and introduce a short perturbence in the image that is a typical signature for the existence of a planet. The largest disadvantage of this method is that a detection can not be reconfirmed, since the alignment of the foreground star with a background star will probably not occur again, and the detected exoplanets are in systems very far away for other methods to observe them.

1.2.2 Direct detection of exoplanets

As the name suggests, direct detection of exoplanets concerns the direct depiction of an exoplanet on an image, separated from its parent star. The direct detection of exoplanets will be the best way to characterize the atmosphere and surface of an Earth–sized exoplanet, with the help of large, ground–based telescopes such

[1]It can be shown that the probability of a planet showing a transit is reversely proportional to its distance from its parent star. Additionally, it can be shown that the depth of the (primary) transit is proportional to the square of the planetary radius, implying that larger planets are easier to detect.

Table 1.1: Number of exoplanet detections by method up to May 2012. Source: The Extrasolar Planets Encyclopaedia (http://exoplanet.eu/).

Method	Number of detections	Number of planetary systems	Number of multiple planetary systems
Radial Velocity	708	563	96
Planetary Transits	231	197	30
Microlensing	15	14	1
Direct Detection	31	27	2

as the European Extremely Large Telescope (E-ELT) (Keller et al. 2010). Since though the planet to star contrast ratio is quite small (see Fig. 1.1), this method is quite challenging. With the aid of polarimetry, the planet to star contrast ratio can be increased by three to four orders of magnitude, making the detection of an exoplanet easier (Keller et al. 2010). Even when the contrast problem is overcome and we manage to observe the exoplanet, we are still faced with the challenge to characterize an exoplanet that is unresolved, i.e. it occupies a single pixel. If the planet resembles the Earth for example, that one single pixel will hold information on oceans, continents, vegetation coverage and cloud content of the planetary atmosphere.

1.3 Characteristic of the planets discovered so far

When we discover an exoplanet with the help of the radial velocity and transit methods, we can get information on its mass and radius and thus we can define its density ($\rho \sim \mathrm{mass}/\mathrm{radius}^3$). The density and radius of a planet can give us an indication of whether this planet is a giant, gaseous planet like Jupiter ($\rho_{\mathrm{J}} \sim$1.33 gr/cm^3) and the rest giants planet of our Solar System or a terrestrial, rocky planet like Earth ($\rho_{\mathrm{J}} \sim$5.51 gr/cm^3) and the rest terrestrial planets of our Solar System.

Most of the exoplanets discovered up to now, are very massive planets, with masses up to a couple of times that of Jupiter, and tend to rotate in very tight orbits around their parent stars (see Fig. 1.3). Thankfully for the researchers interested in finding our Earth's twin, a planet with a size similar to our Earth that lies within its parent star's habitable zone, i.e. the region around the star within which a planet can sustain liquid water on its surface, provided it has an adequate atmosphere (see e.g. Kaltenegger & Sasselov 2011) (see Fig. 1.4), this is not a natural phenomenon making the terrestrial planets of our Solar System unique or special, but an observational bias, intrinsic to the methods and instruments used

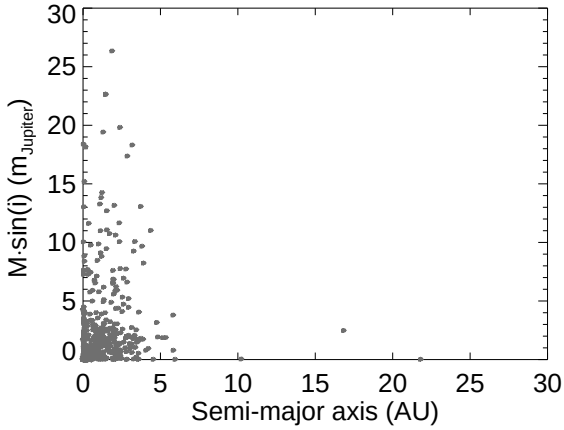

Figure 1.3: A scatter plot of the minimum estimated mass (in Jupiter masses) of the (confirmed) exoplanets detected up to today as a function of the semi–major axis of their orbit (in AU). As we can see, most exoplanets detected up to today are massive objects orbiting in tight orbits around their parent stars.

in the first years of exoplanetary research. In fact, Borucki et al. (2011) comparing the first data from Kepler with ground–based observations have shown that the smaller, terrestrial–like exoplanets should be a lot more common than the large planets, but due to the intrinsic biases of our ground–based methods we have not detected them yet. Recently, Cassan et al. (2012) have estimated that about 62% of the Milky Way stars should actually have an Earth–like planet. Up to today we have detected about five rocky planets, the smallest one of which has a minimum mass of 1.9 $M_{\oplus}$ (Mayor et al. 2009) and its year lasts about 3.15 days. Detecting, and most importantly characterizing even smaller Earth–like exoplanets, will not be possible with the currently used (indirect) methods (Kaltenegger & Traub 2009).

In order to detect and characterize smaller Earth–like exoplanets we need to turn to direct detection of exoplanets, and most particularly in polarization. The disk–integrated light coming to us from distant solar type stars is virtually unpolarized (Kemp et al. 1987). On the other hand, as we will see in Sections 1.5.1 and 1.5.2, the starlight that is reflected by the (exo–)planet will be polarized due to scattering and reflection processes in the planetary atmosphere and surface (when present). Thanks to this, polarization can be used to enhance the planet to star contrast

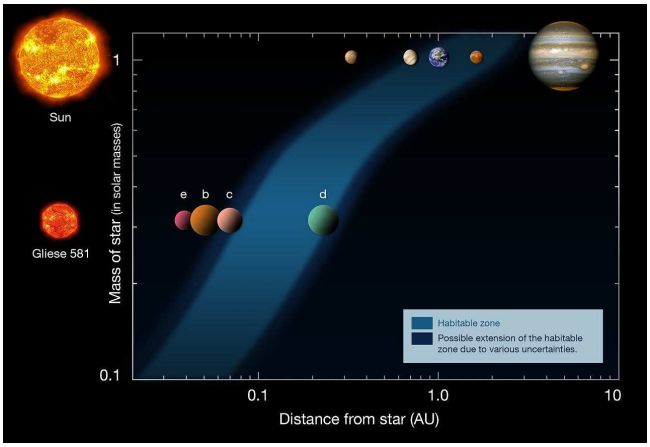

Figure 1.4: Habitable zones of our Sun and Gliese 581. As we can see the hotter the star is, the further away its habitable zone is. Credits: ESO.

ratio by up to three to four orders of magnitude (Keller et al. 2010).

In particular, assume we observe a planetary system in polarization using two mutually perpendicular set–ups of our polarimeter and then we subtract the two images. Since the starlight is unpolarized, its intensity in both images should be approximately the same, thus the subtraction of the two images should leave a (almost) zero signal in the position of the star. Since the planetary light is polarized on the other hand, its intensity will vary between the two images. Assuming that we have chosen the correct orientation for our polarimeter initially, such that the polarimeter is co–alligned with the planet's polarized signal, its perpendicular set–up will allow zero planetary signal passing through and thus the subtraction of the two images will give us the full polarized planetary signal. In this way we can in principal get rid of (most of) the starlight and detect easier the planetary signal (see e.g. Rodenhuis et al. 2011, for an application on a real instrument).

Concluding, in less than two decades thanks to the advancement of our methods and instruments we have detected more than 770 exoplanets. In the next couple of years the number of detected exoplanets will increase exponentially and soon we will find the first Earth–like planets lying in the habitable zone of its parent star. Still though, with the current means we will not be able to properly characterize that exoplanet and we will not be able to make any conclusive remarks on its potential habitability.

1.4 Characterization of exoplanets

With the detection of exoplanets being a routine procedure nowadays, the interest of the exoplanetary community shifts slowly from the plain detection of exoplanets to their characterization. Until the recent past, the planetary characterization involved only the determination of the physical characteristics of the exoplanet, such as its (minimum) mass, radius, density and distance from its parent star. Nowadays though, thanks to our improved instruments and with the aid of transit spectroscopy we can define the chemical content of planetary atmospheres (see e.g. Tinetti et al. 2007, Désert et al. 2011), its atmospheric temperature–pressure profile (see e.g. Huitson et al. 2012, Todorov et al. 2012, Snellen et al. 2010b) and more recently, we can even detect the existence of atmospheric patterns (see e.g. Snellen et al. 2010a).

In the near future, with the detection of the first Earth–like planets, our interest will, inevitably, be shifted towards the detection of signs of habitability. Our experience from our Solar System planets shows that habitability is intertwined with the existence of liquid water on a planetary atmosphere and surface. Detection of liquid water on a planetary atmosphere or surface can be achieved by the detection of the rainbow created by the water clouds on the exoplanetary atmosphere (see Chapters 2, 4 and 6 and references therein), or by the detection of the glint of starlight reflected on liquid surfaces, such as those of oceans, on the exoplanetary surface (see e.g. Williams & Gaidos 2008). In this effort the direct detection of exoplanets and most importantly the use of polarization will provide us with a crucial tool.

1.4.1 Polarization as a tool for the characterization of exoplanets

Polarization is a powerful tool for the characterization of planetary atmospheres and surfaces (Hansen & Travis 1974) that has been known and used in astronomical studies for more than a hundred years. Already in 1929 Lyot (Lyot 1929) was using polarization to study the atmospheres of Venus and Jupiter, while Hansen & Hovenier (1974) were able to derive the composition and size distribution of the droplets on the upper Venusian clouds, as well as the cloud top altitudes in the Venusian atmosphere, thanks to the ability of polarization to brake the degeneracies that the previous flux–only measurements had. In recent years, the power of polarization is generally accepted and applied in studies of Earth's atmosphere and surface for e.g. characterizing aerosols and surfaces and determining the phase (liquid or ice) of water clouds.

Even in the case of the Solar System planets, polarization has proven a valuable

ally (see e.g. Hansen & Hovenier 1974, West et al. 1983, West & Smith 1991, Mishchenko 1993), thanks to its extreme sensitivity to the atmospheric (micro–) physical properties (refractive index of cloud droplets and size distribution, cloud optical thickness and top altitude etc) (Hansen & Travis 1974). This sensitivity being due to the fact that because of the generally low polarization of light that is multiple times scattered in the atmosphere, the main angular features observed in a polarized planetary signal will be due to single scattered light.

Unlike Solar System planets, in the case of exoplanets the planetary signal is disk–integrated. The question arises then if any atmospheric or surface related features can survive in the disk–integration and thus if we can still characterize the planets based on their flux and polarization signals. In the field of terrestrial exoplanets the pioneering work of Ford et al. (2001), and later follow up works of Seager et al. (2005), Stam (2008) and Williams & Gaidos (2008) for example, have shown that the disk integrated signal of exoplanets should preserve crucial information on the planetary composition such as the signal of the so–called red–edge and the ocean glint, while in cases of horizontally homogeneous exoplanets and weighted averaged inhomogeneous exoplanets (the polarization part of) the signal could also hold information on the cloud content of the planetary atmosphere (Stam 2008). In this book, we will show that even in the case of realistically inhomogeneous exoplanets when for example clouds cover just fractions of the planetary surface, their signal can still survive in the disk–integrated polarization, allowing us to "see" their presence in the exoplanetary signal.

But what do we mean when we talk about polarization?

1.5 Defining polarization

Light consists of electric–magnetic waves made out of oscillating and mutually perpendicular electric and magnetic fields which are fully polarized. And while in the case of radio observations measuring waves is possible, the same does not hold for the optical regime studies where we measure photons. Natural, unpolarized light is characterized by the fact that the photons out of which it is made, are polarized in all possible angles, and thus within the normal observing times we cannot track down any "preferred" polarization direction. On the other extreme, a totally linearly polarized light will contain photons polarized all in one and only angle. Generally an arbitrary beam of light of total flux $\pi F_{\rm tot}$ will consist of two parts, an unpolarized part $\pi F_{\rm unpol}$ and a fully polarized part $\pi F_{\rm pol}$, such that $\pi F_{\rm tot} = \pi F_{\rm unpol} + \pi F_{\rm pol}$.

Broad–band polarized light can be created from natural light in four basic ways:

reflection, refraction, differential absorption and scattering. When we are interested in the polarization of starlight reflected of a planet, the reflection (on the planetary surface) and scattering (in the atmosphere) are the two most important processes we deal with.

1.5.1 Polarization due to reflection

When natural light reflects on a surface it will generally become polarized. The extent to which polarization will occur depends on two factors: the angle of incidence (in other words the angle with which the light approaches the surface of the material relevant to the perpendicular) and the material of the surface. For example, most non–metallic surfaces reflect light with one vibrational direction, more efficiently than others (in particular there is a preference to the plane perpendicular to the plane of incidence), thus resulting in polarized light.

When the reflection is regular at the boundary between two media of different refractive indices (for example the atmosphere and the surface) we can describe it using the so–called Fresnel equations (Fresnel 1819).

In general, a surface tends to reflect the incident flux $\pi F_{\rm in}$ anisotropically. The function that is used to describe the way that a surface reflects incident light at various directions is called the *Bidirectional Reflectance Distribution Function (BRDF)* and the function that describes the way the reflected light is polarized at various directions is called the *Bidirectional Polarization Distribution Function (BPDF)*. For modelling Earth surfaces for example, the most common *BPDF* model is that of Nadal & Breon (1999), while a number of models exist for the *BRDF*s (see e.g. Litvinov et al. 2010). These functions tend to take into account the existence of variations on the reflecting surfaces due to e.g. the existence of waves, leaves causing shadowing etc.

A simplified version of the *BRDF* is that of a Lambertian reflector, in which case we assume that the surface reflects the light in the same way in all directions (see Fig. 1.5). The Lambertian approximation, even though not satisfied by any real reflector, is a convenient approximation for many diffuse reflectors (Lenoble 1993).

A basic "disadvantage" of a Lambertian surface is that it is totally depolarizing, i.e. not only it does not polarize light falling on it like surfaces normally do, but even when polarized light falls on it, it will become unpolarized. Studies of the influence of a Lambertian assumption on retrieval algorithms of Earth's atmosphere show that it leads to minor errors (see e.g. O'Dell et al. 2011), but it could introduce some errors in our results when the polarization of reflected light is of interest.

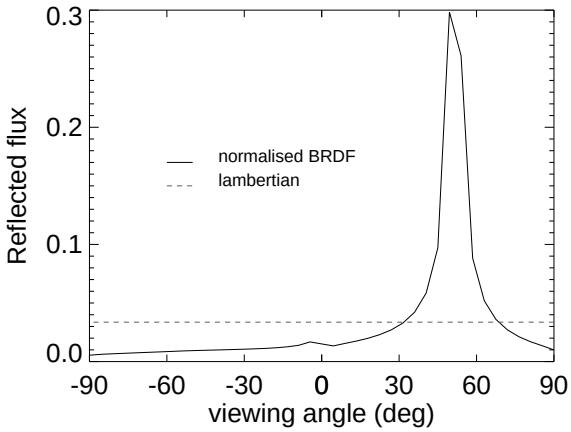

Figure 1.5: Normalized BRDF of a surface versus its lambertian reflection. The input parameters used for the calculation of the BRDF and the albedo of the surface was taken from MODIS data. The normalization of the BRDF is such that the total reflected flux is equal to that of the lambertian case. The solar zenith angle is taken equal to 35°.

1.5.2 Polarization due to scattering

Unpolarized light that travels through an atmosphere and scatters on a particle, generally gets polarized. The reason for this is that as the photons collide with the atoms of the particles it will set them into vibration. In their turn, the vibrating atoms will emit photons that will be radiated in all directions. These waves now can collide with other atoms of the particle, which will reproduce in their turn new photons. In this way the light will be scattered about the medium. This scattered light is polarized (Leroy 2001). The polarization characteristics of the scattered light due to its creation mechanism depends largely on the properties of the scattering particles (in particular its chemical composition, shape, size) and they are wavelength dependent (Stam et al. 2006b).

Assume a beam of light that enters an atmosphere and on its way encounters a particle. If we assume that it undergoes single scattering on it we will get the following pattern for the degree of polarization as a function of the angle. In the back–scattering and forward–scattering directions the degree of polarization will be zero. As we proceed to the perpendicular direction the degree of polarization will increase to higher values, reaching a 100% polarization on the perpendicular

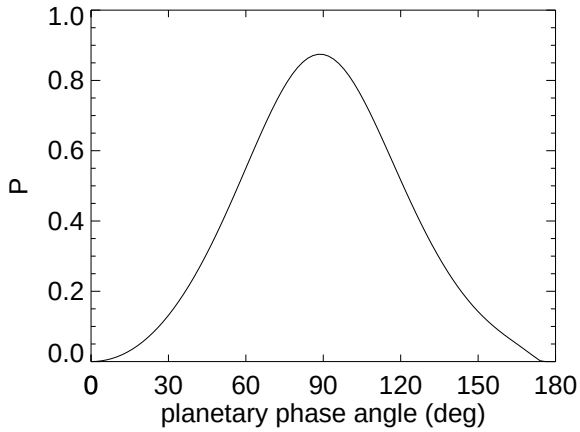

Figure 1.6: P of light reflected by a clear planetary atmosphere keeps the characteristics of the single scattering properties of the atmospheric molecules. Here, we plot P of an ocean planet with a clear, Earth–like atmosphere at 0.65 μm.

(50% if the radiation wavelength is larger than the characteristic dimensions of the scattering particles).

In reality, since the particles are somewhat irregular in shape, and we can be dealing with anisotropic radiation and multiple scattering, the degree of polarization never reaches 100%. This behavior defines to a large degree the "picture" of polarization we get when viewing from above a planetary atmosphere as we can see in Fig. 1.6, where we plot the degree of polarization P as function of the planetary phase angle (α) for an ocean planet with a clear, Earth–like atmosphere.

1.5.3 Stokes formalism

George Gabriel Stokes introduced in 1852 a new way to describe the polarization state of light in the optical regime through intensity measurements, in terms of its total flux (πF), fractional degree of polarization ($P(\lambda)$) and the shape parameters of the polarization ellipse. The Stokes parameters are combined into the Stokes

vector:

$$\pi\vec{F} = \pi \begin{pmatrix} F \\ Q \\ U \\ V \end{pmatrix}, \tag{1.1}$$

which spans the space of all the polarization states of light (namely unpolarized, partially polarized and fully polarized)(Collett 1992). The πF component represents the incoherent sum of the signal (there are no interference effects), the πQ and πU are the differences in linear polarization states at two perpendicular planes and the πV factor represents the circular polarization. In this way for example a light with a Stokes vector of $\pi\vec{F} = (1, 0, 0, 0)$ would be completely unpolarized, while a $\pi\vec{F} = (1, 0, 0, 1)$ would be right-handed, circularly polarized (with respect to the positive x–axis, clockwise as seen by the observer (del Toro Iniesta 2003)).

In the case we are dealing with fully polarized light the total flux will be:

$$F = \sqrt{Q^2 + U^2 + V^2}, \tag{1.2}$$

or in case we are dealing with partial polarized light we will have:

$$F \geq \sqrt{Q^2 + U^2 + V^2}. \tag{1.3}$$

The Degree of polarization (P), the ratio of the flux of the polarized light to the flux of the unpolarized light, as a function of the Stokes parameters is given by:

$$P = \frac{\sqrt{Q^2 + U^2 + V^2}}{F}, \tag{1.4}$$

which in case that $V = 0$ (no circular but only linear polarization) transforms in the degree of linear polarization (P_{L}) that has the form :

$$P_{\mathrm{L}} = \frac{\sqrt{Q^2 + U^2}}{F}. \tag{1.5}$$

When additionally $U = 0$ we define the degree of linear polarization as

$$P_{\mathrm{S}} = -\frac{Q}{F}. \tag{1.6}$$

Based on this we see why as we mentioned earlier, when we have a Stokes vector $\pi\vec{F} = (1, 0, 0, 0)$ we are dealing with unpolarized light, since then we have $P = 0$.

The corresponding Angle of linear polarization (χ) is:

$$\chi = \frac{1}{2}\arctan(\frac{U}{Q}) \tag{1.7}$$

(Hansen & Travis 1974).

1.6 Signals of Earth–like planets

One of the biggest challenges of the field of exoplanets will be the detection and characterization of an Earth–like exoplanet. Particularly, when the first exoplanet with the correct mass and in the correct distance from its parent star is found we will be interested in finding whether this planet has continents and oceans on its surface, and whether there are water clouds in its atmospheres. But how can we figure out what the planetary atmosphere and surface contains?

To decipher the signal of a directly detected exoplanet, we will need numerical models that can simulate single pixel signals of exoplanets with inhomogeneous atmospheres and surfaces (if present). Such models will be essential for the design and optimization of telescope instruments and mission profiles (which are the necessary spectral bands and resolution for characterizing a given object, for how long should we observe etc). Additionally, once the first observations are available, these models can be used to interpret these observations. In order to control our models' ability to characterize an Earth–like exoplanet we need to test them against a planet that has continents, oceans and water clouds on its atmosphere, i.e. our Earth. But what can we expect when we will observe an Earth–like exoplanet?

In Fig. 1.7 we present calculated disk–integrated flux and polarization spectrum of our Earth as an exoplanet for a phase angle of 46° or 90° and for various Earth configurations. The continuum features we see in Fig. 1.7, which as we see vary with the phase angle, are due to the various surface and atmospheric features of Earth. For example, we notice that the lower albedo of the ocean surface when the Pacific is in the center of our field of view, leads to a lower reflected flux (and correspondingly higher polarization) than in the case Eurasia and Africa are on the center of our field of view.

In the latter case we notice a bump for wavelengths longer than 0.65 μm, which is the so–called red–edge caused by the vegetation that is in our field of view. Unlike what our eyes would tell us, vegetation on Earth tends to reflect a lot more light around 0.7μm (the near infrared part of the spectrum) than around 0.5μm, the wavelength area that gives plants their distinctive green color. In particular, if we would plot the vegetational reflectivity as a function of wavelength, the region of

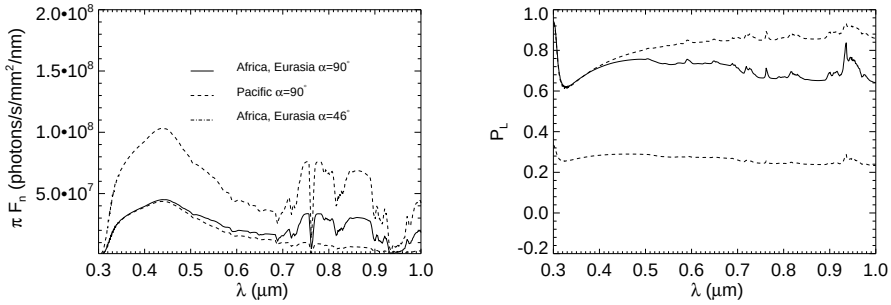

Figure 1.7: Calculated flux πF (left) and degree of linear polarization $P_{\rm L}$ (right) of sunlight reflected by the Earth as functions of λ, for $\alpha = 90^{\circ}$: with Africa and Eurasia in view and no clouds (solid lines), with the Pacific ocean in view and no clouds (dashed lines) and for for $\alpha = 46^{\circ}$ with Africa and Eurasia in view (dashed-dotted lines).

the visual spectrum from about 0.6μm onwards would present an increase up to five times or more in comparison to the 0.5μm region. This sudden increase in the reflectivity is called the *red edge*. The exact location and intensity of this red edge depends on the nature of the vegetation and its environment (see Seager et al. 2005, and references therein).

In Fig. 1.7 we have treated the ocean surface as a black surface, and thus the only effect it has on our signal is due to its lower albedo. In reality though the ocean surface can have a larger influence to the total planetary signal at specific phase angles through the so–called *glint*. In particular, a liquid surface such as a planet's oceans can reflect light in a mirror–like way causing the glint. In case the liquid surface is flat (e.g. a non–waved ocean) the angle of reflectance equals the angle of incidence and we have a normal *specular reflection*. Specular reflection of starlight on a planetary ocean can affect its polarization properties, making the light highly polarized. In case the liquid surface is wavy, foamy etc, things can be more complicated but a number of analytical solutions exist to describe the flux and polarization properties of the reflected light (Nadal & Breon 1999, Martin 2004).

The high spectral resolution features that we see in both flux and polarization are due to gaseous absorption bands. At the shortest wavelengths light is absorbed by the atmospheric O_3, causing a dip in the reflected flux and a corresponding increase in the degree of polarization around 0.3 μm. Between $\sim$0.5 μm and $\sim$0.7μm we notice, especially in the case we observe areas with high surface albedo

(here, the case of Africa and Eurasia), a dip in the reflected flux, which is the so–called Chappuis absorption band of O_3. Around 0.76 μm we notice a deep absorption band which is the famous oxygen A–band, the easiest identifiable O_2 band in our atmosphere. The oxygen A–band is useful for the characterization of planetary atmospheres, since its depth compared to the continuum, can help us determine the cloud top heights in a planetary atmosphere (see e.g. Wu 1985, and references therein).

In polarization, we notice that the spectrum of our planet looks similar to that in flux, only now the absorption lines have transformed into "emission" lines, i.e. there is a local increase in the degree of polarization where an absorption line lies. The reason for this is that the absorption of light in a band decreases the amount of multiple scattered light and we see mostly light that is singly scattered ((normally) with a higher degree of polarization) in the atmosphere.

The general increase in polarization that we observe with wavelength is due to the decrease in the optical thickness of the atmosphere with wavelength, which leads to a small(er) amount of multiple scattering. In this way, in the case we observe the Pacific region, since the ocean surface is almost black the polarization reaches almost as high as the single scattering value of the atmosphere. In the case we observe the Africa–Eurasia area on the other hand, a number of photons will have managed to reach as low as the surface and get reflected. At the longer wavelengths, where the atmosphere is less opaque the number of photons that have managed to penetrate the atmosphere and reflect on the surface is (getting) comparable to the number of singly scattered photons on the upper atmosphere and the degree of polarization decreases.

1.6.1 Looking for the rainbow

"It's a trick of the light"

– Mike Oldfield, *Discovery, 1984*

An important feature to look for when we are interested in the detection of water clouds on exoplanets is the *rainbow* (see e.g. Bailey 2007, and references therein). The rainbow of water clouds is formed by light that has been refracted and reflected one or more times inside their water particles (see van de Hulst 1957, Adam 2002, Bailey 2007). The dispersion of the colors in a rainbow is due to the different refractive index that materials exhibit for photons of different wavelengths, a phenomenon known as *(chromatic) dispersion*. Short–wavelength (blue) light is refracted at a greater angle than long–wavelength (red) light.

The rainbow that we are all most familiar with, is the result of two refractions and one reflection inside the water droplets and is known as the *primary rainbow*. Due to the reflection of the light inside the droplet, the blue light will emerge at a smaller angle to the incident white light than the red light, causing blue to be on the inside of a rainbow arc and red on the outside. A less frequently observed rainbow, is that caused by light that has been reflected twice inside the water particles, the so–called *secondary rainbow*. Due to the second reflection its colors are reversed in comparison to the primary rainbow, i.e. the red color appears on the inside of the rainbow–arc and the blue color on the outside. Due to the angle of (incidence or) reflection being equal to the Brewster angle in the case of water droplets, the reflected light will be (almost) completely perpendicularly polarized, giving the primary and secondary rainbows high degrees of polarization (the primary rainbow can reach a P =96% and the secondary rainbow a P =90% (see Adam 2002, and references therein)). In principal, more than two internal reflections can take place inside each droplet, causing the so–called tertiary, quaternary and higher order rainbows (Adam 2002).

Rainbows' angular position depends strongly on the refractive index of the scattering particles and slightly on their radius ($r_{\rm eff}$) (see Chapter 2 and Adam (2002)). In Fig. 1.8, we plot the degree of linear polarization ($P_{\rm S}$) of starlight scattered by a planetary atmosphere as a function of wavelength (λ) and the planetary phase angle (α). The color coding indicates the various values of $P_{\rm S}$. In the left plot our model planet has a cloud deck of water clouds in its atmosphere and on the right plot a cloud deck of sulfuric acid (H_2SO_4), like Venus. The bump of higher $P_{\rm S}$ around α =30°– 40° that we see in the left plot is the primary rainbow (notice how the location of the peak changes as a function of λ). As we can see a similar feature does not appear in the case of H_2SO_4.

In this book we will look for the rainbow on exoplanets with cloud decks and cloud patches. Especially in Chapter 4 we will try to find the limits within which the rainbow can still give us insight on the existence of water on the planetary atmosphere, depending on the cloud coverage and the existence of ice clouds in the planetary atmosphere.

We should finally note here, that while the rainbow we are all most familiar with on Earth is caused by large, water drops, the rainbows we are interested in in this book are made by the interaction of starlight with water cloud particles, whose size many times does not exceed 10 μm (0.00001 meters).

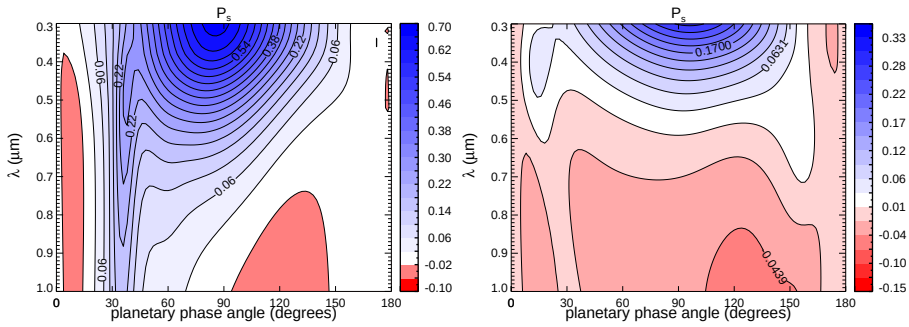

Figure 1.8: Degree of polarization $P_{\rm S}$ as function of the planetary phase angle α and the wavelength λ for two cloud decked planets. Left plot: the cloud deck is made of water clouds, Right plot: the cloud deck is made of sulfuric acid. The primary rainbow (that we can see as an increase in $P_{\rm S}$ between $\alpha = 30^\circ$ and $\alpha = 40^\circ$) is apparent in the case of the water clouds, but non visible in the case of the sulfuric acid clouds.

1.7 Modelling the signals of exoplanets

As we previously mentioned, to decipher the signal of a directly detected exoplanet, we will need numerical models that can simulate single pixel signals of exoplanets with inhomogeneous atmospheres and surfaces (if present). Such models will be essential for the design and optimization of telescope instruments and mission profiles (which are the necessary spectral bands and resolution for characterizing a given object, for how long should we observe etc). Additionally, once the first observations are available, these models can be used to interpret these observations.

A number of models exist today that are used to calculate the signals of starlight reflected by gaseous and terrestrial exoplanets (see e.g. Ford et al. 2001, Tinetti 2006, Williams & Gaidos 2008, Stam 2008). Most of them treat only the flux and ignore the polarization, a fact that can introduce large errors in our interpretation of our observations (see e.g. Stam & Hovenier 2005). In a few cases that the models do take polarization into account, they tend to do it over–simplified (for example ignoring multiple scattering), or if they take polarization properly into account they treat homogeneous only planets.

Most of the planets of our Solar System though, exhibit some form of inhomogeneity or another (oceans, continents, (liquid or ice) water clouds, ammonia ice clouds, zones, belts and spots etc.). To mimic this inhomogeneity, some of the models that treated homogeneous–only planets used methods like the *weighted*

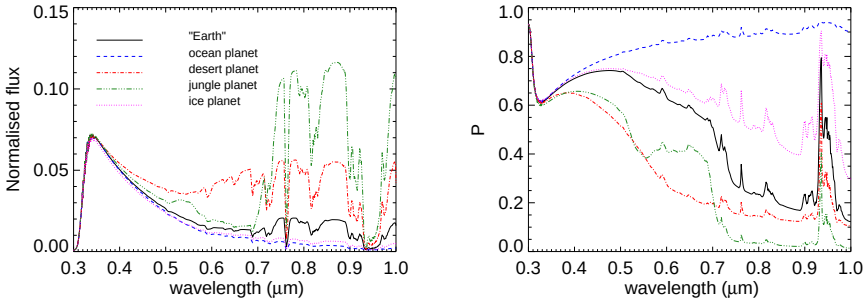

Figure 1.9: An example of how the weighted averaging method works. Our simplified Earth–as–an–exoplanet is covered by ∼72% by ocean, ∼10% by desert, ∼9.4% by forest and ∼8.6% by ice. Our model "Earth" is observed at a phase angle of 90°.

averaging (Stam 2008), in which the flux and polarization signals of a number of homogeneous planets are (weighted) summed up to create the inhomogeneous planetary signal. The weight given to each one of the homogeneous models depends on the percentage coverage on the planet of the feature treated in the model. For example, to model the signal of a simplified and cloudless Earth–as–an–exoplanet, we would need to use a model of an ocean world (a planet covered completely by water), a desert world, a jungle world and an ice world. Then knowing that at a random time the Earth is covered by e.g. ∼72% by ocean, ∼10% by desert, ∼9.4% by forest and ∼8.6% by ice we can produce the total Earth–as–an–exoplanet signal by adding 0.72·(ocean world signal) + 0.10·(desert world signal) + 0.094·(jungle world signal) + 0.086·(ice world signal) (see Fig. 1.9). Of course, the question arises how good is this approximation, and which are the limits within which we can use it without large deviations from the "truth".

In this book, we will present a new numerical code that can deal with truly horizontally and vertically inhomogeneous exoplanets and can produce their full, disk–integrated flux and polarization signal as a function of the observational wavelength and the planetary phase angle (i.e. where the planet lies on its orbit around its parent star). Our code is based on the same efficient and accurate adding–doubling algorithm as Stam et al. (2004) and can take polarization properly into account (all orders of scattering, all kinds of different clouds, surface reflection etc). As we will show later on this book, the results from our "truly" inhomogeneous planets show that the *weighted averaging* cannot be used for the complete characterization of exoplanets, unless the latter are almost homogeneous. In par-

ticular, the lack of information that the *weighted averaging* method has on the geographical distribution of inhomogeneities on the planet affects to a large degree the predicted flux and polarization spectra of the model exoplanets.

1.8 Instruments for polarimetric studies of exoplanets

A number of instruments are being planned that will use polarimetry as a method to detect and characterize exoplanets. In the next couple of years the Spectro-Polarimetric High-contrast Exoplanet Research (SPHERE) (see Beuzit et al. 2006) instrument on the Very Large Telescope (VLT) of ESO in Chile will increase the number of directly detected (giant) exoplanets. SPHERE consists of three instruments, IRDIS (Infra-Red Dual-beam Imager and Spectrograph), IFS (Infra-red Integral Field Spectrograph) and ZIMPOL (Zurich IMaging POLarimeter). The first two instruments will work on detecting exoplanets in the infrared part of the spectrum (above 0.95 μm), while ZIMPOL will work on characterizing detected exoplanets with the help of polarization in the visible part of the spectrum (0.6 μm to 0.9 μm) (Povel et al. 1994). IRDIS includes a dual polarimetric imaging mode (DPI) for imaging extended stellar environments (e.g. detecting disks of dust).

Another instrument that should see light within the next years is the Gemini Planet Imager (GPI) (Macintosh et al. 2006), which will target the characterization of giant planets observing between 0.9 μm and 2.4 μm. GPI will use polarization measurements to measure the polarization of light to see faint disks of dust from other solar systems' comet and asteroid belts (Perrin et al. 2010).

In the further future the Exoplanet Imaging Camera and Spectrograph (EPICS) (see Kasper et al. 2010) and its polarization instrument EPOL (Exoplanet PO-Larimeter) on the European Extremely Large Telescope (E–ELT) will push the limits of the lowest mass of *directly* detected and characterized exoplanets down to massive terrestrial objects and will aim to detect terrestrial planets located in the habitable zone of their parent star (see Kasper et al. 2010, Keller et al. 2010). EPOL will operate in the visible part of the spectrum between 0.6 μm (target 0.5 μm) and 0.9 μm.

An innovative concept for the direct detection and characterization of exoplanet is that of the New Worlds Observer (NWO) (Cash & New Worlds Study Team 2010). NWO plans on using a large occulter in front of a space telescope to block the light of nearby stars in order to observe their orbiting planets. Another instrument moving along similar lines is the Telescope for Habitable Earth and Interstellar/Intergalactic Astronomy (THEIA) (Seager et al. 2009). THEIA is designed to be a multi-instrument space-telescope concept for a 4–m diffraction-

limited telescope operating at UV/visible wavelengths. While NWO will use polarization for the detection and characterization of exoplanets similar plans do not exist for THEIA so far.

We should note here that the use of polarimetry in missions like these is important not only because it can help us detect an exoplanet easier (Keller et al. 2010), but also because it helps us *correctly* characterize an exoplanet. In particular, experience from Earth observations shows that not taking polarization into account, even when we are interested in flux only measurements, can introduce large errors in our interpretations of our observations (see e.g. Natraj et al. 2007, Sromovsky 2005).

As preparation for these missions and to test our models to a first order, we perform Earthshine observations, i.e. we study the light that gets reflected by the day side Earth on the Moon and back to us (see e.g. Turnbull et al. 2006, Sterzik et al. 2012). Unfortunately though, while such measurements are helpful there may still be some intrinsic biases that we cannot properly correct for (like for example the exact effect of the lunar surface on the polarization properties of the reflected Earthlight). For a proper control of our models we would ideally need direct observations of Earth as an exoplanet.

An interesting instrument concept that can help us on this, and that we will discuss further in Chapter 6 is that of LOUPE, the Lunar Observer for Unresolved Polarimetry of Earth. LOUPE is a small, lightweight instrument that could be placed on a lunar lander to observe the Earth as if it were an exoplanet. Thanks to the monthly orbit of the Moon around the Earth and its tidal locking with respect to the Earth, an instrument like LOUPE on a Lunar Lander could observe the whole of the Earth, all of the time and at all phase angles, from about 0° (i.e. a fully illuminated Earth disk), up to about 180° (i.e. a fully dark Earth disk). In this way, already in a months time LOUPE would see the Earth going through all the variations that (almost) any other Earth–like exoplanet that we could observe and characterize would go through. Ideally, the mission should last long enough to cover all seasons and capture the effects of seasonal changes (local solar zenith angles, weather and cloud patters, surface albedos, polar nights etc). An instrument like LOUPE would create a benchmark dataset against which we could test our retrieval models and which could be used for reference on every future Earth–like exoplanet characterization.

This thesis is organized as follows:

In Chapter 2 we study the case of horizontally homogeneous planets, completely covered by liquid water clouds. Our planets are vertically inhomogeneous, i.e. every atmospheric layer can have a different composition of the other ones. We study the effect of a number of cloud micro– and macro–physical properties on the planetary flux and polarization signal. Our aim in this chapter is to explore the information content of the spectropolarimetric signal of cloudy planets and the wavelength and phase angle ranges that can provide use with most information on the atmospheric content.

In Chapter 3 we present the code we developed that can treat horizontally and vertically inhomogeneous planets. We test our code against the previously well–tested horizontally homogeneous code we used in Chapter 2. We then study the validity of the previously used *weighted averaging* method (see Chapter 1.7). We find that while the latter method can give us a feeling for the nature of inhomogeneities met on a planet (for example through the rainbow and its location), it can lead to errors on the characterization of the exoplanet since it holds no information on the location of inhomogeneities on the planetary surface. We apply our new code to some first test cases, using terrestrial exoplanets with atmospheric and/or surface inhomogeneities.

In Chapter 4 we study horizontally and vertically inhomogeneous planets with patchy water clouds and try to look for signs of the rainbow under various coverage and multi–cloud–layer conditions. We see that the rainbow is visible in polarization for planets with a cloud coverage above 10% for observation at 0.55 μm (20% for observation at 0.865 μm), while the existence of ice clouds can mask the existence of water clouds (and the rainbow) only for the cases the ice clouds overcast more than half of the water clouds. Using MODIS/Aqua data for Earth, we model a simplified exo–Earth with liquid water and ice clouds and test whether an alien observer would notice the liquid water clouds in our planetary atmosphere.

In Chapter 5 we modify our code to study the effect of various inhomogeneities on the signal of gaseous, giant (exo–)planets. We study the effect that various inhomogeneities that occur on the giant planets of our Solar System (bands, spots, polar haze etc) have on the planetary signal. We notice that polarization is more sensitive than flux to the existence of these inhomogeneities. For example, while the variation in the signal of a Jupiter–like planet due to the diurnal rotation of a spot is non measurable in flux, in polarization it leaves a distinctive trace. In some cases more than one inhomogeneities could cause a similar variation on the planetary signal. The existence of multi–wavelength observations could help us distinguish between the various cases.

In Chapter 6 we use our code to study a model of Earth–as–an–exoplanet and present LOUPE, the Lunar Observatory for Unresolved Polarimetry of Earth. LOUPE is a small and lightweight instrument that could be placed on a lunar lander like ESA's Lunar Lander that will be launched in 2018 (if selected). From the Moon LOUPE will be able to make benchmark observations of Earth as if it were an exoplanet, that will be very valuable for future characterization of Earth–like exoplanets.

Finally, in Chapters 7 and 8 we present a summary of the research presented in this thesis in Dutch and Greek.